

Magnetic phases of the mixed-spin $J_1 - J_2$ Heisenberg model on a square lattice

N.B. Ivanov¹, J. Richter², and D.J.J. Farnell³

¹⁾ *Max-Planck Institut für Physik Komplexer Systeme, Nöthnitzer Str. 38, D-01187 Dresden, Germany**

²⁾ *Institut für Theoretische Physik, Universität Magdeburg, PF 4120, D-39016 Magdeburg, Germany*

³⁾ *School of Mechanical Engineering, University of Leeds, Woodhouse Lane Leeds LS2 9JT, United Kingdom*
(December 2, 2024)

We study the zero-temperature phase diagram and the low-energy excitations of a mixed-spin ($S_1 > S_2$) $J_1 - J_2$ Heisenberg model defined on a square lattice by using a spin-wave analysis, the coupled cluster method, and the Lanczos exact-diagonalization technique. As a function of the frustration parameter J_2/J_1 (> 0), the phase diagram exhibits a quantized ferrimagnetic phase, a canted spin phase, and a mixed-spin collinear phase. The presented results point towards a strong disordering effect of the frustration and quantum spin fluctuations in the vicinity of the classical spin-flop transition. In the extreme quantum system (S_1, S_2) = $(1, \frac{1}{2})$, we find indications of a new quantum spin state in the region $0.46 < J_2/J_1 < 0.5$.

PACS: 75.10.Jm, 75.50.Gg, 75.40.Gb, 75.40.-s

There has recently been an increasing interest in Heisenberg spin systems exhibiting quantum phases with an extensive magnetic moment. An intriguing example is the bilayer Hall system at filling factor $\nu = 2$ which was shown to possess a canted spin state with spontaneously broken $U(1)$ symmetry.^{1,2} A closely related phase diagram was studied in the framework of the bilayer quantum Heisenberg model subject to a perpendicular magnetic field.³ Some specific properties of the quantum phase transitions in systems with quantum ferromagnetic phases have been previously discussed by using a special class of lattice models with quantum-rotor degrees of freedom.⁴ In the present paper we study a $J_1 - J_2$ Heisenberg model which is a natural (mixed-spin) extension of the well known antiferromagnetic $J_1 - J_2$ model⁵ and exhibits most of the quantum magnetic phases found in the aforementioned rotor systems.

The model is defined by the Hamiltonian

$$\mathcal{H} = J_1 \sum_{(\mathbf{r}, \mathbf{r}')} \mathbf{S}_{1\mathbf{r}} \cdot \mathbf{S}_{2\mathbf{r}'} + J_2 \sum_{[\mathbf{r}, \mathbf{r}']} (\mathbf{S}_{1\mathbf{r}} \cdot \mathbf{S}_{1\mathbf{r}'} + \mathbf{S}_{2\mathbf{r}} \cdot \mathbf{S}_{2\mathbf{r}'}), \quad (1)$$

where $(\mathbf{r}, \mathbf{r}')$ and $[\mathbf{r}, \mathbf{r}']$ denote pairs of nearest and next-nearest (diagonal) sites of the square lattice. We choose a checkerboard arrangement for the spin operators $\mathbf{S}_{1\mathbf{r}}$ and $\mathbf{S}_{2\mathbf{r}}$ [$\mathbf{S}_{1\mathbf{r}}^2 = S_1(S_1 + 1)$, $\mathbf{S}_{2\mathbf{r}}^2 = S_2(S_2 + 1)$, and $S_1 > S_2$] and introduce the parameters $\alpha \equiv J_2/J_1$ ($J_1, J_2 \geq 0$) and $\sigma \equiv S_1/S_2$. With some minor modifications, e.g., introducing a spatial anisotropy in the nearest-neighbor exchange interaction, the Hamiltonian (1) could describe a large class of real mixed-spin compounds such as the bimetallic molecular magnets.⁶

In the classical limit the phase diagram of the mixed-spin system contains the ferrimagnetic state (F phase), the canted state (C phase), and the mixed-spin collinear state⁷ (N phase) shown in Fig. 1. The latter phases are stable, respectively, in the parameter regions $\alpha < \alpha_{c1}$, $\alpha_{c1} < \alpha < 0.5$, and $\alpha > 0.5$. The classical F-C tran-

sition at $\alpha_{c1} = (2\sigma)^{-1}$ is continuous, whereas the C-N transition at $\alpha = 0.5$ is connected with a flop of the S_1 and S_2 spins. The canted spin phase appears as a result of the magnetic frustration without explicit breaking of the $SU(2)$ symmetry (in the mentioned bilayer systems the C phase is generated by a perpendicular magnetic field). Note also that the S_2 spins remain collinear in the C phase. The angle θ measuring the local orientation of the classical S_1 spins in respect to the global magnetization axis z alternatively takes the values

$$\theta = \pm \arccos \frac{1}{2\alpha\sigma}. \quad (2)$$

Bimetallic molecular magnets are normally characterized by small exchange constants J_1 such that the canted phase may appear for a moderate magnetic frustration provided that the parameter σ is large enough.

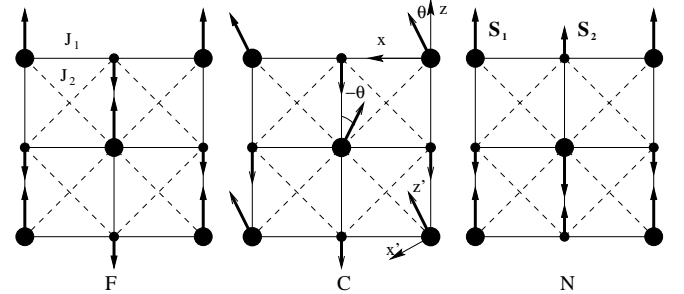


FIG. 1. The classical ferrimagnetic (F), canted (C), and collinear (N) spin phases of the mixed-spin $J_1 - J_2$ model on a square lattice.

In this article we study the quantum phase diagram of the model (1) by using the standard spin-wave theory (SWT), the coupled cluster method⁸ (CCM), and the Lanczos exact-diagonalization (ED) technique.

To perform a SWT analysis we assume that the classical spins lie in the xz plane. Using as a quantization axis

the local orientation of the classical spins (the z' axis in Fig. 1), the leading spin-wave terms in the expansions for the spin operators $\mathbf{S}_{1\mathbf{r}}$ and $\mathbf{S}_{2\mathbf{r}}$ read

$$\begin{aligned} S_{i\mathbf{r}}^z &= \cos \theta_{i\mathbf{r}} (S_i - a_{i\mathbf{r}}^\dagger a_{i\mathbf{r}}) - \sin \theta_{i\mathbf{r}} \sqrt{\frac{S_i}{2}} (a_{i\mathbf{r}}^\dagger + a_{i\mathbf{r}}), \\ S_{i\mathbf{r}}^x &= \sin \theta_{i\mathbf{r}} (S_i - a_{i\mathbf{r}}^\dagger a_{i\mathbf{r}}) + \cos \theta_{i\mathbf{r}} \sqrt{\frac{S_i}{2}} (a_{i\mathbf{r}}^\dagger + a_{i\mathbf{r}}), \\ S_{i\mathbf{r}}^y &= i \sqrt{\frac{S_i}{2}} (a_{i\mathbf{r}}^\dagger - a_{i\mathbf{r}}) \quad (i = 1, 2), \end{aligned}$$

where the angle $\theta_{i\mathbf{r}}$ measures the local deviations of z' from the magnetization axis z . A substitution of the latter expressions in Eq. (1) yields the following spin-wave Hamiltonian written in terms of the Fourier transforms $a_{i\mathbf{k}}$ of the boson operators $a_{i\mathbf{r}}$:

$$\begin{aligned} \mathcal{H}_0 &= \sum_{i=1}^2 \sum_{\mathbf{k}} \left[A_{i\mathbf{k}} a_{i\mathbf{k}}^\dagger a_{i\mathbf{k}} + \frac{B_{i\mathbf{k}}}{2} (a_{i\mathbf{k}}^\dagger a_{i-\mathbf{k}}^\dagger + a_{i\mathbf{k}} a_{i-\mathbf{k}}) \right] \\ &+ \sum_{\mathbf{k}} \left[C_{\mathbf{k}} a_{1\mathbf{k}}^\dagger a_{2-\mathbf{k}}^\dagger + D_{\mathbf{k}} a_{1\mathbf{k}}^\dagger a_{2\mathbf{k}} + h.c. \right] + E_0. \quad (3) \end{aligned}$$

Note that E_0 is the energy of the classical spin state; the coefficients in Eq. (3) are defined below. The wave vector $\mathbf{k} = k_1 \mathbf{e}_1 + k_2 \mathbf{e}_2$ runs in the paramagnetic Brillouin zone (PBZ) $|k_1 \pm k_2| \leq \pi/a_0$ (the unit vectors $\mathbf{e}_1 \perp \mathbf{e}_2$ point towards the main directions on the square lattice). We shall henceforth use a system of units where the lattice spacing $a_0 = 1$.

The canonical transformation

$$a_{i\mathbf{k}} = \sum_{j=1}^2 \left[u_{i\mathbf{k}}^{(j)} \alpha_{j\mathbf{k}} + v_{i\mathbf{k}}^{(j)} \alpha_{j-\mathbf{k}}^\dagger \right] \quad (i = 1, 2)$$

recasts \mathcal{H}_0 to the diagonal form

$$\mathcal{H}_0 = E_0 - \sum_{\mathbf{k}} A_{\mathbf{k}} + \sum_{i=1}^2 \sum_{\mathbf{k}} \omega_i(\mathbf{k}) \left(\alpha_{i\mathbf{k}}^\dagger \alpha_{i\mathbf{k}} + \frac{1}{2} \right), \quad (4)$$

where $A_{\mathbf{k}} = (A_{1\mathbf{k}} + A_{2\mathbf{k}})/2$. In the PBZ any of the discussed magnetic phases is characterized by two branches of spin-wave excitations $[\omega_i = \omega_i(\mathbf{k}), i = 1, 2]$

$$\omega_{1,2} = \sqrt{F_{\mathbf{k}} \mp \sqrt{G_{\mathbf{k}}}}, \quad (5)$$

where $F_{\mathbf{k}} = (\epsilon_{1\mathbf{k}}^2 + \epsilon_{2\mathbf{k}}^2)/2 + D_{\mathbf{k}}^2 - C_{\mathbf{k}}^2$, $G_{\mathbf{k}} = (\epsilon_{1\mathbf{k}}^2 - \epsilon_{2\mathbf{k}}^2)^2/4 + (\epsilon_{1\mathbf{k}}^2 + \epsilon_{2\mathbf{k}}^2)(D_{\mathbf{k}}^2 - C_{\mathbf{k}}^2) + 2(A_{1\mathbf{k}}A_{2\mathbf{k}} + B_{1\mathbf{k}}B_{2\mathbf{k}})(C_{\mathbf{k}}^2 + D_{\mathbf{k}}^2) - 4(A_{1\mathbf{k}}B_{2\mathbf{k}} + A_{2\mathbf{k}}B_{1\mathbf{k}})C_{\mathbf{k}}D_{\mathbf{k}}$, and $\epsilon_{i\mathbf{k}} = (A_{i\mathbf{k}}^2 - B_{i\mathbf{k}}^2)^{1/2}$ ($i = 1, 2$). ω_1 and ω_2 are the positive solutions of the biquadratic algebraic equation

$$\Delta(\omega) \equiv \det \hat{\mathcal{D}}(\omega) = 0. \quad (6)$$

The dynamical matrix $\hat{\mathcal{D}}(\omega)$ reads

$$\hat{\mathcal{D}}(\omega) = \begin{bmatrix} A_{1\mathbf{k}} - \omega & B_{1\mathbf{k}} & D_{\mathbf{k}} & C_{\mathbf{k}} \\ B_{1\mathbf{k}} & A_{1\mathbf{k}} + \omega & C_{\mathbf{k}} & D_{\mathbf{k}} \\ D_{\mathbf{k}} & C_{\mathbf{k}} & A_{2\mathbf{k}} - \omega & B_{2\mathbf{k}} \\ C_{\mathbf{k}} & D_{\mathbf{k}} & B_{2\mathbf{k}} & A_{2\mathbf{k}} + \omega \end{bmatrix}.$$

A straightforward calculation gives the following expression for the on-site magnetizations $m_1 \equiv \langle S_{1\mathbf{r}}^{z'} \rangle$ and $m_2 \equiv \langle S_{2\mathbf{r}}^{z'} \rangle$:

$$m_i = S_i - \frac{2}{N} \sum_{\mathbf{k}} \left[|v_{i\mathbf{k}}^{(1)}|^2 + |v_{i\mathbf{k}}^{(2)}|^2 \right] \quad (i = 1, 2), \quad (7)$$

where

$$\begin{aligned} v_{1\mathbf{k}}^{(1)} &= -\frac{\Delta_{12}(\omega_1)}{\sqrt{2\omega_1(\omega_2^2 - \omega_1^2)\Delta_{11}(\omega_1)}}, \\ v_{2\mathbf{k}}^{(1)} &= \frac{-\Delta_{14}(\omega_1)}{\sqrt{2\omega_1(\omega_2^2 - \omega_1^2)\Delta_{11}(\omega_1)}}, \\ v_{1\mathbf{k}}^{(2)} &= \sqrt{\frac{-\Delta_{11}(-\omega_2)}{2\omega_2(\omega_2^2 - \omega_1^2)}}, \\ v_{2\mathbf{k}}^{(2)} &= \frac{-\Delta_{13}(-\omega_2)}{\sqrt{-2\omega_2(\omega_2^2 - \omega_1^2)\Delta_{11}(-\omega_2)}}. \end{aligned} \quad (8)$$

$\Delta_{ij}(\omega)$ is the minor of the ij element of $\Delta(\omega)$ in the above expressions.

Phase diagram:

The phase diagram of the extreme quantum system $(1, \frac{1}{2})$ in terms of the on-site magnetizations m_1 and m_2 , Eq. (7), is presented in Fig. 2. The ferrimagnetic phase is characterized by the net ferromagnetic moment per cell $M_0 = (S_1 - S_2) = \frac{1}{2}$. The latter is supposed to be oriented along the z axis. In the general case it is straightforward to observe that M_0 takes only integer or half-integer values. Following the authors of Ref. 4, this state may be referred to as a *quantized unsaturated ferromagnetic phase*. In addition, the F phase is characterized by the on-site magnetizations $m_1 \neq 0$ and $m_2 \neq 0$. ED data show that the position of the continuous phase transition α_{c1} is slightly changed by quantum fluctuations towards larger α .

More important changes take place in the C phase. The canted spin state is additionally characterized by the staggered transverse field $\langle S_{1\mathbf{r}}^x \rangle = m_1 \sin \theta \neq 0$ which breaks the spin rotation symmetry $U(1)$ in the xy plane. Note that in the C phase the combined disordering effect of the magnetic frustration and quantum spin fluctuations is strongly enhanced as compared to the F phase. SWT predicts a complete magnetic disordering of the S_2 spins ($m_2 = 0$) starting at the point α^* (see Fig. 2). α^* precedes the classical spin-flop transition point ($\alpha = 0.5$) and exists in the SWT for arbitrary spins S_1 and S_2 . The latter effect is strongly pronounced in the extreme quantum case $(1, \frac{1}{2})$ where both the SWT and the ED data predict $\alpha^* \approx 0.46$. The extrapolated CCM data seem to show the same tendency. The steps in the ED data in Figs. 2 and 3 are a pure finite-size effect and reflect the change in the total spin S_t (a good quantum number) of

the absolute ground state with the frustration parameter J_2/J_1 . For instance, in the ED data α^* appears as a point where S_t changes from $S_t = 1$ to $S_t = 0$. Although SWT formally predicts $m_1 > 0$ even beyond α^* , the latter region is not accessible (for the standard SWT) as the phase with $m_1 > 0$ and $m_2 = 0$ does not appear in the classical phase diagram.⁹ We suggest that the point α^* is just the position of the quantum spin-flop transition (see below).

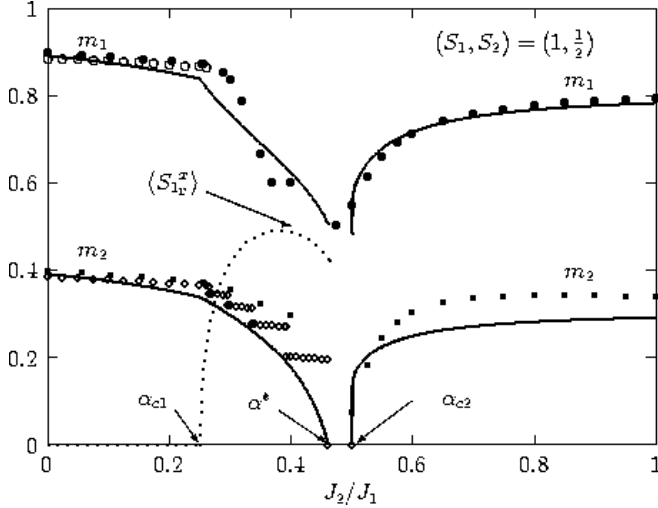


FIG. 2. The on-site magnetizations $m_1 = \langle S_{1r}^z \rangle$ and $m_2 = \langle S_{2r}^z \rangle$ plotted as a function of J_2/J_1 : SWT (full lines), CCM (filled circles), ED for $N = 20$ spins and periodic boundary conditions (open circles). The dashed line represents the SWT result for the transverse condensate $\langle S_{1r}^x \rangle$.

Finally, the mixed-spin collinear state has properties which are similar to those of the collinear phase in the antiferromagnetic $J_1 - J_2$ model, i.e., it is a Néel-type magnetic state characterized by the on-site magnetizations $m_1, m_2 \neq 0$. Both the SWT and the CCM predict that the on-site magnetization m_2 vanishes at a point (α_{c2}) which is very close to the classical spin-flop transition point.

The ED data for different spin-spin correlations give some additional evidence in favor of the suggested phase diagram (see Fig. 3). Here the phase transition point α_{c2} can be indicated as a point where the mixed-spin correlations (being ferromagnetic in the N phase) change their sign. We observe that close to the point α_{c2} the spin-spin correlations among the S_2 spins are small and also change their sign. On the other hand, the correlations among the S_1 spins remain relatively large (and antiferromagnetic, as in the N phase) down to the point $\alpha^* \approx 0.46$, where the singlet ground state disappears. Thus, there are some indications that the established quantum spin phase ($\alpha^* < \alpha < \alpha_{c2}$) has the symmetries of the canonical Néel state composed of S_1 spins (i.e., $m_1 \neq 0, m_2 = 0$). However, due to the finite-size

effects in the ED data we can not exclude the spin-liquid state ($m_1 = 0, m_2 = 0$) as a possible ground state in the above region. Further understanding of the proposed phase diagram may be achieved by studying the low-lying excitations in these magnetic phases.

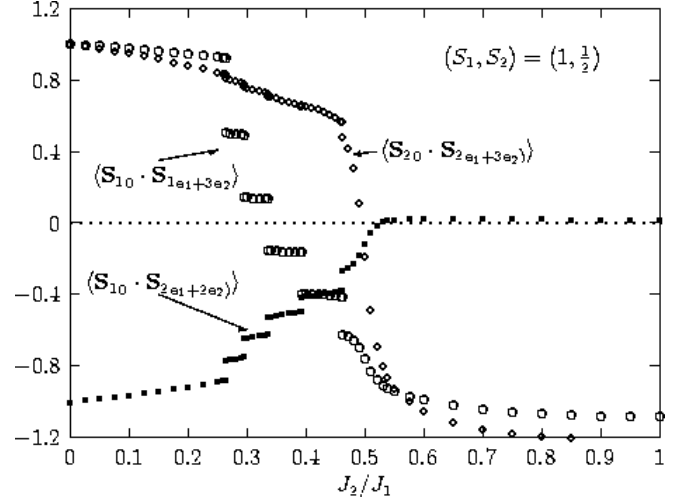


FIG. 3. Spin-spin correlators vs. J_2/J_1 in the system with $N = 20$ spins (ED results). The presented functions are scaled by their absolute values at $J_2 = 0$.

Low-energy excitations:

In the F phase $B_{1\mathbf{k}} = B_{2\mathbf{k}} = D_{\mathbf{k}} = 0$ and the dispersion relations in Eq. (5) are simplified to

$$\omega_{1,2}^{(F)} = \sqrt{A_{\mathbf{k}}^2 - C_{\mathbf{k}}^2} \pm \frac{1}{2}(A_{1\mathbf{k}} - A_{2\mathbf{k}}), \quad (9)$$

where $A_{1\mathbf{k}} = 4J_1S_2 - 4J_2S_1(1 - \nu_{\mathbf{k}})$, $A_{2\mathbf{k}} = 4J_1S_1 - 4J_2S_2(1 - \nu_{\mathbf{k}})$, $C_{\mathbf{k}} = 4J_1\sqrt{S_1S_2}\gamma_{\mathbf{k}}$, $\nu_{\mathbf{k}} = \cos k_1 \cos k_2$, and $\gamma_{\mathbf{k}} = (\cos k_1 + \cos k_2)/2$. The low-energy physics is controlled by the acoustic branch $\omega_1^{(F)}$. For small $|\mathbf{k}|$ $\omega_1^{(F)}$ takes the form

$$\omega_1^{(F)} = \frac{\rho_s^{(F)}}{m_0}k^2 + \mathcal{O}(k^4), \quad (10)$$

where $\rho_s^{(F)} = J_1S_1S_2 - J_2(S_1^2 + S_2^2)$ is the spin-stiffness constant of the ferrimagnetic state and $m_0 = (S_1 - S_2)/a^2$ ($a = \sqrt{2}$) is the magnetization density. $\rho_s^{(F)}$ remains finite at the F-C transition point α_{c1} . The F-C phase transition is connected with a softening of the acoustic branch $\omega_1^{(F)}$ at the corners of the PBZ. For instance, close to $\mathbf{k} = (0, \pi)$ the magnon spectrum reads

$$\omega_1^{(F)} = 8J_1S_1(\alpha_{c1} - \alpha) + 4J_1S_1[k_1^2 + (\pi - k_2)^2].$$

On the other hand, the optical branch $\omega_2^{(F)}$ remains stable at α_{c1} and does not play important role in the quantum F-C phase transition.

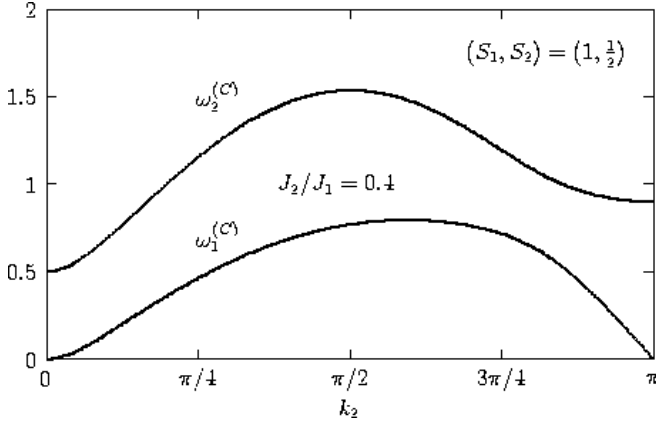


FIG. 4. Spin-wave spectrum in the C phase along the \mathbf{e}_2 direction of the PBZ ($k_1 = 0$, $J_1 \equiv 1$).

The excitation spectrum in the C phase is described by the general expression (5), where $A_{1\mathbf{k}} = 4J_1S_2t + 4J_2S_1[1 - t^2(2 - \nu_{\mathbf{k}})]$, $A_{2\mathbf{k}} = 4J_1S_1t - 4J_2S_2(1 - \nu_{\mathbf{k}})$, $B_{1\mathbf{k}} = -4J_2S_1(1 - t^2)\nu_{\mathbf{k}}$, $B_{2\mathbf{k}} = 0$, $C_{\mathbf{k}} = 2J_1\sqrt{S_1S_2}(1 + t)\gamma_{\mathbf{k}}$, $D_{\mathbf{k}} = -2J_1\sqrt{S_1S_2}(1 - t)\gamma_{\mathbf{k}}$, and $t^{-1} = 2\sigma\alpha$ (see Fig. 4). As may be expected, in addition to the quadratic spin-wave excitations, Eq. (10), close to the zone corners there appear linear Goldstone excitations connected to the spontaneously broken $U(1)$ symmetry in the C phase. For example, in the vicinity of $\mathbf{k} = (0, \pi)$ the spectrum takes the form

$$\omega_1^{(C)} = v\sqrt{k_1^2 + (\pi - k_2)^2}, \quad v = 4J_1S_1\sqrt{\alpha^2 - \alpha_{c1}^2}.$$

Note that the spin-wave velocity v vanishes at the F-C transition point α_{c1} .

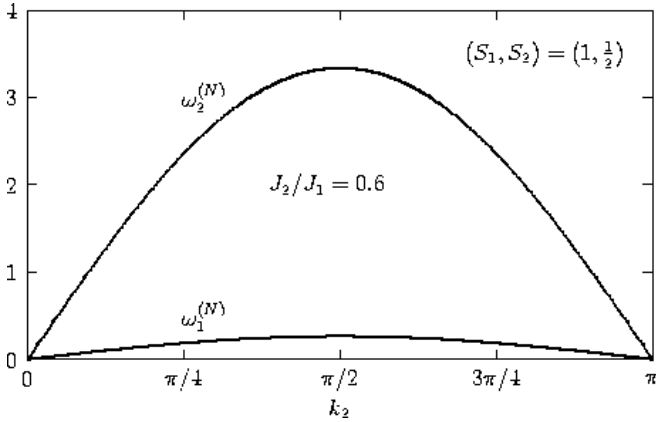


FIG. 5. Spin-wave spectrum in the N phase along the \mathbf{e}_2 direction of the PBZ ($k_1 = 0$, $J_1 \equiv 1$).

Finally, the spin-wave spectrum in the mixed-spin collinear phase is given by the general relation (5), where $A_{1\mathbf{k}} = 4J_2S_1$, $A_{2\mathbf{k}} = 4J_2S_2$, $B_{1\mathbf{k}} = 4J_2S_1\nu_{\mathbf{k}}$, $B_{2\mathbf{k}} = 4J_2S_2\nu_{\mathbf{k}}$, $C_{\mathbf{k}} = 2J_1\sqrt{S_1S_2}\cos k_2$, and $D_{\mathbf{k}} =$

$2J_1\sqrt{S_1S_2}\cos k_1$ (see Fig. 5). As compared to the antiferromagnetic $J_1 - J_2$ model, the excitation spectrum in the mixed-spin collinear phase shows some important peculiarities which specify the instability at the classical transition point $\alpha = 0.5$. First, in the mixed-spin system the degeneracy of the spin-wave branches $\omega_1^{(N)}$ and $\omega_2^{(N)}$ is completely removed. Second, the spin-wave excitations described by $\omega_2^{(N)}$ formally remain stable down to the point $\alpha = \sqrt{\sigma}/(\sigma + 1)$ [$= \sqrt{2}/3 \approx 0.47$ for the $(1, \frac{1}{2})$ system]. The phase transition at α_{c2} is entirely driven by instabilities in the lower $\omega_1^{(N)}$ excitation branch. At the classical spin-flop transition point ($\alpha = 0.5$), the branch $\omega_1^{(N)}$ exhibits two full lines of zero modes (i.e., $k_1 = 0$ and $k_2 = 0$) in the PBZ. The soft lines are connected with *ferromagnetic* fluctuations in the \mathbf{e}_1 and \mathbf{e}_2 directions on the square lattice, so that we can expect that quantum fluctuations do not change the position of the classical transition point (in accord with the data presented in Fig. 2).¹⁰

In conclusion, we have studied the quantum spin phases in the mixed-spin $J_1 - J_2$ Heisenberg model defined on a square lattice. The reported results support a phase diagram with an additional quantum spin phase close to the classical spin-flop transition. In the extreme quantum case $(1, \frac{1}{2})$, we have found indications of a quantum spin phase (in the region $0.46 < \alpha < 0.5$) which is characterized by magnetically disordered S_2 spins and Néel long-range ordered S_1 spins. However, the adopted methods can not exclude the spin-liquid state as a possible ground state. A study with other analytical and numerical methods would be necessary to characterize the true ground state in the above region.

This work was partially supported by the Bulgarian Science Foundation (Grant No. 817/98) and the Deutsche Forschungsgemeinschaft (Grant NO. Ri615/7-1).

* Permanent address: Institute of Solid State Physics, Bulgarian Academy of Sciences, Tzarigradsko chaussee 72, 1784 Sofia, Bulgaria.

¹ S. Das Sarma, S. Sachdev, and L. Zheng, Phys. Rev. B **58**, 4672 (1998), and references therein.

² At filling factor $\nu = 2$ the system can be mapped onto the spin- $\frac{1}{2}$ easy-plane Heisenberg ferromagnetic model subject to a magnetic field along the z direction: K. Yang, Phys. Rev. B **60**, 15 578 (1999).

³ Y. Matsushita, M. Gelfand, and C. Ishii, J. Phys. Soc. Jpn. **66**, 3648 (1997); M. Troyer and S. Sachdev, Phys. Rev. Lett. **81**, 5418 (1998).

⁴ S. Sachdev, Z. Phys. B **94**, 469 (1994); S. Sachdev and T. Senthil, Ann. Phys. (NY) **251**, 76 (1996).

⁵ see, e.g., O.P. Shushkov, J. Oitmaa, and Z. Weihong,

Phys. Rev. B **63**, 104420 (2001).

⁶ O. Kahn, *Molecular magnetism* (VCH, New York, 1993).

⁷ The classical N phase is degenerate in respect to global rotations of the S_1 (or S_2) subsystem. Quantum fluctuations choose one of the collinear configurations corresponding to ferromagnetic spin arrangements along the \mathbf{e}_1 or the \mathbf{e}_2 directions on the square lattice.

⁸ Below we present extrapolated results obtained with the SUB m - m approximation scheme ($m = 2, 4$, and 6 in the F and N phases; $m = 3, 4$, and 5 in the C phase): see D.J.J. Farnell, K.A. Gernoth, and R.F. Bishop, Phys. Rev. B **64**, 172409 (2001).

⁹ The region beyond α^* can be studied in the framework of the modified spin-wave theories: M. Takahashi, Phys. Rev.

B **40**, 2494 (1989); J.E Hirsch and S. Tang, Phys. Rev. B **40**, 4769 (1989); Q.F Zhong and S. Sorela, Europhys. Lett. **21**, 629 (1993).

¹⁰ Note that in the classical mixed-spin collinear phase the chain configurations in the \mathbf{e}_2 direction are characterized with a finite ferromagnetic moment per cell. As a result, the soft line $k_1 = 0$ in the mixed-spin state is connected with ferromagnetic spin fluctuation. The above moments are zero in the uniform-spin ($S_1 = S_2$) collinear phase, so that the soft line $k_1 = 0$ is connected with antiferromagnetic fluctuations. This explains the change of the position of the α_{c2} point ($\alpha_{c2} \approx 0.6$) found in the spin- $\frac{1}{2}$ $J_1 - J_2$ Heisenberg model.